Resolvable Group Target Tracking via Multi-Bernoulli Filter and Its Application to Sensor Control Scenario

Guchong Li, *Member, IEEE*, Gang Li, *Senior Member, IEEE*, and You He

***Abstract*—In this paper, we address the problem of resolvable group target tracking (RGTT) and the application of RGTT in the sensor control scenarios. The aim of our approach is to further improve the tracking performance of multi-Bernoulli (MB) filter by exploiting the group structure information. Firstly, a single-target state transition function (SSTF) is derived from the direct integral solution of the single-target state stochastic differential equation (SDE), which is used to revise the prediction process of the standard MB filter. Then, combing the Gaussian mixture (GM) implementation, the prediction process of the proposed SSTF-based MB (SSTF-MB) filter is detailed. Next, considering the benefits and importance of group structure in the sensor control scenarios, the proposed SSTF-MB filter is applied into a mobile sensor platform whose control actions (e.g., motion direction) are uncertain. Specifically, the proposed SSTF-MB filter is merged into a sensor control strategy where the Cauchy-Schwarz (CS) divergence is selected as the objective function to compute the discrepancy between two first-order moment approximations of MBs. Finally, the efficiency and performance of the proposed SSTF-MB filter and its application to sensor control scenario is well demonstrated in the simulation experiments.**

***Index Terms*—Cauchy-Schwarz divergence, multi-Bernoulli, resolvable group target tracking, sensor control, single-target state transition function.**

NOMENCLATURE

List of Acronyms

CPHD	Cardinalized Probability Hypothesis Density
CS	Cauchy-Schwarz
GC	Gaussian Component
GLMB	Generalized Labeled Multi-Bernoulli
GM	Gaussian Mixture
GSTF	Group-center State Transition Function
JPDAF	Joint Probabilistic Data Association Filter
JSTFD	Joint-target State Transition Function Decomposition
JSTFD-MB	JSTFD-based MB
KL	Kullback-Leibler
LMB	Labeled Multi-Bernoulli
MB	Multi-Bernoulli
MC	Monte Carlo
MCMC	Markov Chain Monte Carlo
MHT	Multiple Hypothesis Tracker
OSPA	Optimal Sub-Pattern Assignment
PEECS	Posterior Expected Error of Cardinality and States
PHD	Probability Hypothesis Density
PIMS	Predicted Ideal Measurement-Set
POMDP	Partially Observable Markov Decision Process
PPP	Poisson Point Process
RFS	Random Finite Set
RGTT	Resolvable Group Target Tracking
RS-SSTF-MB	Random Selection based on SSTF-MB
SC-MB	Sensor Control based on MB
SC-SSTF-MB	Sensor Control based on SSTF-MB
SDE	Stochastic Differential Equation
SMC	Sequential Monte Carlo
SSTF	Single-target State Transition Function
SSTF-MB	SSTF-based MB
TOGC	Translational Offset of the Group Center
TOGC-MB	TOGC-based MB

Manuscript received 3 July 2022; revised 30 October 2022; accepted 8 January 2023. Date of publication 11 January 2023; date of current version 19 January 2023. The associate editor coordinating the review of this manuscript and approving it for publication was Prof. Ba Ngu Vo. This work was supported in part by the National Key R&D Program of China under Grant 2021YFA0715201, in part by the National Natural Science Foundation of China under Grants 61925106, 62022092, 62293544, and 62201316, and in part by Chinese Postdoctoral Science Foundation under Grant 2022M711872. *(Corresponding author: Gang Li.)*

Guchong Li and Gang Li are with the Department of Electronic Engineering, Tsinghua University, Beijing 100084, China (e-mail: guchong.li@hotmail.com; gangli@tsinghua.edu.cn).

You He is with the Institute of Information Fusion, Naval Aviation University, Yantai 264001, China, and also with the Department of Electronic Engineering, Tsinghua University, Beijing 100084, China (e-mail: heyou@mail.tsinghua.edu.cn).

Digital Object Identifier 10.1109/TSP.2023.3236158

I. INTRODUCTION

RESOLVABLE group target is defined as a set of targets whose motion models interact with each other, meanwhile, each target occupies a resolution unit. In the *resolvable group target tracking* (RGTT) scenarios, the group structure performs a significant role in the multi-target Bayes filtering process [1]. Thus, it is necessary for the RGTT, comparing to the traditional multi-target tracking approaches, to consider the group structure during the tracking process to further improve the tracking performance.

In general, the group structure, which depends on the placement of targets within the group, is diverse. For example, a circular formation model, where one target is at the center of

a circle and other targets make up the circle, is proposed in [2], and the tree structure with fixed relative positions in the group are exploited in [3], [4], [5]. As a matter of fact, the movement of tracking objects is always flexible, such as tracking pedestrians and drone swarm. For such cases, the visual leader-follower model wherein the member is the *translational offset of the group center* (TOGC) can be adopted [6], but a more general approach to model the group structure relationship is using *stochastic differential equation* (SDE). Pang et al. utilize SDEs to characterize the group structure wherein the position, velocity, force and noise are considered at the same time, meanwhile, a *Markov chain Monte Carlo* (MCMC) particles algorithm is adopted to perform sequential inference [7]. Moreover, a computationally efficient algorithm is proposed in [8]. Further, the SDE is also used in the leader-follower model and its effectiveness is verified by the practical pigeon flocking data [9], [10].

A currently difficult topic, but one worth exploring, is how to deal with the RGTT problem under some challenging scenarios, such as unknown and time-varying number of targets and groups. For this issue, the filters based on *random finite set* (RFS) theory, comparing to *joint probabilistic data assoication filter* (JPDAF) [11] and *multiple hypothesis tracker* (MHT) [12], are more attractive. *Probability hypothesis density* (PHD) filter is an effective RFS-based filtering tool via only propagating the first-order moment of multi-target states [13]. *Cardinalized PHD (CPHD)* filter [14], comparing to the PHD filter, propagates both first-order moment and cardinality distribution. Instead of propagating the moments and cardinality distributions, *multi-Bernoulli* (MB) filter [15] propagates the parameters of a MB distribution to approximate the posterior multi-target density. Besides, some labeled RFS filters. e.g., *generalized labeled multi-Bernoulli* (GLMB) [16], [17] and *labeled multi-Bernoulli* (LMB) [18], are also proposed to output complete trajectories. In the practical scenes, the selection of filters always depends on the specific tracking requirement. For example, the unlabeled RFS filters may be more popular when the identities of interested targets are unnecessary/unimportant, e.g., car collision avoidance system.

Recently, a new filtering approach, wherein the *joint-target state transition function decomposition* (JSTFD) is performed, is proposed to solve the RGTT problem by taking advantage of both SDE-based group structure and RFS-based filter [19]. This approach utilizes the graph theory to estimate the group structure [20] and derives a single-target state transition equation, which is very convenient for the implementation of prediction process. However, the derivation of repulsive force vector is approximately obtained by first-order Taylor to the positions, meanwhile, the process noise during the prediction process is also not considered.

Note that the aforementioned works either for multi-target tracking or for RGTT assume that the sensor is static. For some tracking scenarios with mobile sensors such as airborne radar, sensor control needs to be considered along with the tracking process. Generally speaking, the sensor control problem is often tackled via formulating the stochastic process as a *partially observable Markov decision process* (POMDP) [21], [22], and the aim is to select the optimized solution from the objective function. From the viewpoint of designing the objective function, there are two main sensor control strategies:

- *Task-based approaches:* The objective function is formulated by considering a performance metric, such as variance of state and cardinality estimates [23], [24], [25], *posterior expected error of cardinality and states* (PEECS) [26], [27], and *optimal sub-pattern assignment* (OSPA) distance [28]. However, these methods only focus on addressing one metric while the other metrics may perform poorly. When multiple performance metrics need to be considered, the weight aggregation of different performance metrics can be adopted, but how to select the weight remains a challenge.
- *Information-based approaches:* It is a direct manner to obtain a superior overall performance by measuring the divergence between the predicted and updated multi-target distributions, which can avoid the weight aggregation. The most common divergence functions include *Kullback-Leibler* (KL) divergence [29], Renyi divergence [23], [30], [31], [32] and *Cauchy-Schwarz* (CS) divergence [33], [34], [35], [36], [37], [38]. In most cases, the KL and Renyi divergences always need significant computational cost, and meanwhile, they cannot be computed analytically. Moreover, it needs to emphasize that the CS divergence has been proved to support the closed form for PHDs [33] and GLMBs [38], which avoids resorting to sampling tools and reduces the computational burden. Besides, the CS divergence are also successfully explored in some multi-sensor control scenarios [39], [40], [41].

However, the current works mainly focus on the multi-target tracking without considering the group structure. As far as we know, the sensor control problem in the RGTT scenarios has not been addressed yet.

Considering the characteristics of easy to estimate the group structure due to inherent separation of individual target estimates comparing to PHD/CPHD filters and low computational cost for scenarios where the identities of targets are not important comparing to LMB/GLMB filters, the MB filter is selected as the filtering tool. Hereafter, the MB-based RGTT and its application to the sensor control scenarios are explored. The main contributions of the paper are concluded as follows:

1) *We propose a MB filter based on the single-target state transition function (SSTF), abbreviated as SSTF-MB, wherein the group structure information is considered in the prediction process.* First of all, by integrating the single-target state SDE, a SSTF is derived but the result is coupled to the state of group center. To solve this problem, we further derive a *group-center state transition function* (GSTF) by summing all SSTFs. Next, combing the derived SSTF and *Gaussian mixture* (GM) implementation tool, the prediction process of the proposed SSTF-MB filter is detailed.[1]
2) *We propose an effective sensor control strategy based on the SSTF-MB filter named SC-SSTF-MB.* Since the prediction process depends on the group structure and

[1]The update process of the proposed SSTF-MB filter is similar to that of the standard MB filter [15], so only the prediction process is introduced later.

plays an important role in the sensor control strategy, thus, we firstly provide a 6-tuple discrete-time POMDP in which the group structure information is added into the SSTF. Next, the detailed SC-SSTF-MB filter is described where the proposed SSTF-MB filter is adopted and the discrepancy between two MB RFSs is evaluated by their first-order moment approximations in terms of CS divergence.

The remainder of the paper is organized as follows. Section II introduces the background knowledge. Sections III and IV describe the proposed SSTF-MB filter and SC-SSTF-MB filter. In Section V, the effectiveness of the proposed SSTF-MB filter and SC-SSTF-MB filter is verified in two RGTT scenarios. Finally, the conclusions are drawn in Section VI.

II. Background

This section provides some background knowledge, including multi-target Bayes recursion, standard MB filter, SDE-based group structure and CS divergence.

A. Multi-Target Bayes Recursion

In this paper, the states and measurements in the single-target systems are modeled by lower case letters (e.g., x and z) while the states and measurements in the multi-target systems are modeled by upper case letters (e.g., X and Z). Suppose that there are N targets and M measurements, and then, the multi-target state and multi-target measurement are, respectively, modeled as the following two RFSs:

$$X = \left\{x^{(1)}, \ldots, x^{(N)}\right\} \subset \mathcal{X}, \tag{1}$$

$$Z = \left\{z^{(1)}, \ldots, z^{(M)}\right\} \subset \mathcal{Z}, \tag{2}$$

where $\mathcal{X}$ and $\mathcal{Z}$ denote the state space and measurement space, respectively.

Given the multi-target density[2] $\pi_t(X)$ at time t and multi-target transition function $T_{t+\tau|t}(\cdot|\cdot)$ from time t to time $t+\tau$ where τ is the sampling rate, the predicted multi-target distribution at time $t+\tau$, denoted as $\pi_{t+\tau|t}(X)$, is computed by the Chapman-Kolmogorov equation [42]

$$\pi_{t+\tau|t}(X_{t+\tau}) = \int T_{t+\tau|t}(X_{t+\tau}|X)\pi_t(X)\delta X. \tag{3}$$

Given a new measurement set at time $t+\tau$, denoted as $Z_{t+\tau}$, the updated multi-target distribution is computed via a multi-target Bayes rule:

$$\pi_{t+\tau}(X_{t+\tau}|Z_{t+\tau}) = \frac{L_{t+\tau}(Z_{t+\tau}|X_{t+\tau})\pi_{t+\tau|t}(X_{t+\tau})}{\int L_{t+\tau}(Z_{t+\tau}|X)\pi_{t+\tau|t}(X|Z_{t+\tau})\delta X}, \tag{4}$$

where $L_{t+\tau}(Z_{t+\tau}|X_{t+\tau})$ is the multi-target measurement likelihood function at time $t+\tau$.

[2]Here, for simplification, the history measurement sets before time t are omitted.

Note that the involved integrals in (3) and (4) are the set integral [42] defined by

$$\int f(X)\delta X = \sum_{n=0}^{\infty} \frac{1}{n!} \int_{X^n} f(\{x^{(1)}, \ldots, x^{(n)}\}) dx^{(1)} \cdots dx^{(n)}. \tag{5}$$

B. Standard MB Filter

A Bernoulli RFS X has an existence probability r and a state density $p(x)$ [1], and its distribution is defined by

$$\pi(X) = \begin{cases} 1-r, & X = \emptyset \\ rp(x), & X = \{x\} \\ 0, & \text{otherwise.} \end{cases} \tag{6}$$

A MB RFS X is a union of multiple independent Bernoulli RFSs $X^{(i)}, i \in \{1, \ldots, N\}$, i.e., $X = \cup_{i=1}^{N} X^{(i)}$. The parameter $r^{(i)}$ denotes the existence probability of the i-th target and parameter $p^{(i)}(x)$ denotes the probability density of the state conditioned on its existence. Therefore, the MB RFS is completely characterized by MB parameters $\{(r^{(i)}, p^{(i)})\}_{i=1}^{N}$. Moreover, the first-order moment of MB RFS is given by

$$D(x) = \sum_{i=1}^{N} r^{(i)} p^{(i)}(x), \tag{7}$$

where $D(x)$ is also named intensity function or PHD [43].

Next, the standard MB filter recursion [15] is given by the following standard prediction and update steps.

1) Standard Prediction: Assume that the posterior multi-target density at time t is MB given by

$$\pi_t = \left\{(r_t^{(i)}, p_t^{(i)})\right\}_{i=1}^{N_t}, \tag{8}$$

then the predicted multi-target density at time $t+\tau$ is MB given by a union of newborn targets and predicted targets,

$$\begin{aligned} \pi_{t+\tau|t} = & \left\{(r_{P,t+\tau|t}^{(i)}, p_{P,t+\tau|t}^{(i)})\right\}_{i=1}^{N_t} \\ & \cup \left\{(r_{\Gamma,t+\tau}^{(i)}, p_{\Gamma,t+\tau}^{(i)})\right\}_{i=1}^{N_{\Gamma,t+\tau}}, \end{aligned} \tag{9}$$

where

$$r_{P,t+\tau|t}^{(i)} = r_t^{(i)} \left\langle p_t^{(i)}, P_{S,t+\tau} \right\rangle, \tag{10a}$$

$$p_{P,t+\tau|t}^{(i)}(x) = \frac{\left\langle f_{t+\tau|t}(x|\cdot), p_t^{(i)} P_{S,t+\tau} \right\rangle}{\left\langle p_t^{(i)}, P_{S,t+\tau} \right\rangle}, \tag{10b}$$

$P_{S,t+\tau}(\cdot)$ denotes the survival probability, $\langle \cdot, \cdot \rangle$ is the inner product computation meaning $\langle f, g \rangle = \int f(x)g(x)dx$, and $f_{t+\tau|t}(x|\cdot)$ denotes the SSTF.

2) Standard Update: Assume that the predicted multi-target density at time $t+\tau$ is MB given by

$$\pi_{t+\tau|t} = \left\{(r_{t+\tau|t}^{(i)}, p_{t+\tau|t}^{(i)})\right\}_{i=1}^{N_{t+\tau|t}}, \tag{11}$$

then the updated posterior multi-target density by a measurement set $Z_{t+\tau}$ at time $t+\tau$ is a union of legacy and updated

components,

$$\pi_{t+\tau} \approx \left\{\left(r_{L,t+\tau}^{(i)}, p_{L,t+\tau}^{(i)}\right)\right\}_{i=1}^{N_{t+\tau|t}} \cup \left\{\left(r_{U,t+\tau}(z), p_{U,t+\tau}(\cdot;z)\right)\right\}_{z\in Z_{t+\tau}}, \tag{12}$$

where

$$r_{L,t+\tau}^{(i)} = r_{t+\tau|t}^{(i)} \frac{1-\left\langle p_{t+\tau|t}^{(i)}, P_{D,t+\tau}\right\rangle}{1-r_{t+\tau|t}^{(i)}\left\langle p_{t+\tau|t}^{(i)}, P_{D,t+\tau}\right\rangle}, \tag{13a}$$

$$p_{L,t+\tau}^{(i)}(x) = p_{t+\tau|t}^{(i)}(x) \frac{1-P_{D,t+\tau}(x)}{1-\left\langle p_{t+\tau|t}^{(i)}, P_{D,t+\tau}\right\rangle}, \tag{13b}$$

$$r_{U,t+\tau}(z) = \frac{\sum_{i=1}^{N_{t+\tau|t}} \frac{r_{t+\tau|t}^{(i)}(1-r_{t+\tau|t}^{(i)})\left\langle p_{t+\tau|t}^{(i)}, g_{t+\tau}(z|\cdot)P_{D,t+\tau}\right\rangle}{\left(1-r_{t+\tau|t}^{(i)}\left\langle p_{t+\tau|t}^{(i)}, g_{t+\tau}(z|\cdot)P_{D,t+\tau}\right\rangle\right)^2}}{\kappa_{t+\tau}(z) + \sum_{i=1}^{N_{t+\tau|t}} \frac{r_{t+\tau|t}^{(i)}(1-r_{t+\tau|t}^{(i)})\left\langle p_{t+\tau|t}^{(i)}, g_{t+\tau}(z|\cdot)P_{D,t+\tau}\right\rangle}{1-r_{t+\tau|t}^{(i)}\left\langle p_{t+\tau|t}^{(i)}, g_{t+\tau}(z|\cdot)P_{D,t+\tau}\right\rangle}}, \tag{13c}$$

$$p_{U,t+\tau}(x;z) = \frac{\sum_{i=1}^{N_{t+\tau|t}} \frac{r_{t+\tau|t}^{(i)}}{1-r_{t+\tau|t}^{(i)}} p_{t+\tau|t}^{(i)} g_{t+\tau}(z|x) P_{D,t+\tau}(x)}{\sum_{i=1}^{N_{t+\tau|t}} \frac{r_{t+\tau|t}^{(i)}}{1-r_{t+\tau|t}^{(i)}} \left\langle p_{t+\tau|t}^{(i)}, g_{t+\tau}(z|\cdot)P_{D,t+\tau}\right\rangle}, \tag{13d}$$

$P_{D,t+\tau}(\cdot)$ and $g_{t+\tau}(z|\cdot)$ denote the detection probability and single-target likelihood function, respectively, and $\kappa_{t+\tau}(\cdot)$ is the intensity of Poisson clutter at time $t+\tau$.

C. SDE-Based Group Structure

Considering a group consisting of N targets, the state of the i-th ($i \in \{1,\ldots,N\}$) target at time t is denoted as $x_t^{(i)} = [p_{t,x}^{(i)}, v_{t,x}^{(i)}, p_{t,y}^{(i)}, v_{t,y}^{(i)}]^\top$ where '$\top$' is the transpose operation, $p_{t,x}^{(i)}$ and $v_{t,x}^{(i)}$ denote the position and velocity in the x direction, respectively, $p_{t,y}^{(i)}$ and $v_{t,y}^{(i)}$ denote the position and velocity in the y direction, respectively. Moreover, the single-target motion in terms of the velocity in the x direction is modeled by the following SDE [7], [44]:

$$dv_{t,x}^{(i)} = \left\{-\alpha\Delta p_{t,x}^{(i)} - \gamma v_{t,x}^{(i)} - \beta\Delta v_{t,x}^{(i)} + r_{t,x}^{(i)}(p_{t,x}^{(i)})\right\} dt + dW_{t,x}^{(i,v)} + dB_{t,x}^{v}, \tag{14}$$

where α and β are positive and reflect the strength of the pull towards the group center, the term $\gamma v_{t,x}^{(i)}$ prevents the velocity becoming very large over time, $W_{t,x}^{(i,v)}$ models the individual randomness of each target in the group while $B_{t,x}^{v}$ models the overall randomness in the motion of the group,

$$\Delta p_{t,x}^{(i)} = p_{t,x}^{(i)} - f\left(p_{t,x}\right), \Delta v_{t,x}^{(i)} = v_{t,x}^{(i)} - g\left(v_{t,x}\right) \tag{15}$$

denote the differences of position and velocity between the individual target and group center. Moreover,

$$f\left(p_{t,x}\right) = \frac{1}{N}\sum_{i=1}^{N} p_{t,x}^{(i)}, g\left(v_{t,x}\right) = \frac{1}{N}\sum_{i=1}^{N} v_{t,x}^{(i)} \tag{16}$$

denote the position and velocity of group center, and $r_{t,x}^{(i)}(p_{t,x})$ denotes the repulsive force acting on target i by other targets in the same group on the x-axis,

$$r_{t,x}^{(i)}(p_{t,x}) = \sum_{\forall k, k\neq i} r_{t,x}^{(k,i)} = \sum_{k\neq i} \frac{f_t^{(k,i)}}{d_t^{(k,i)}}(p_{t,x}^{(k)} - p_{t,x}^{(i)}), \tag{17}$$

where

$$f_t^{(k,i)} = \frac{R_1}{d_t^{(k,i)} + R_2}, \tag{18}$$

R_1 and R_2 are the parameters controlling the magnitude of $f_t^{(k,i)}$, and $d_t^{(k,i)}$ denotes the distance between target i and target k at time t,

$$d_t^{(k,i)} = \sqrt{\left(p_{t,x}^{(k)} - p_{t,x}^{(i)}\right)^2 + \left(p_{t,y}^{(k)} - p_{t,y}^{(i)}\right)^2}. \tag{19}$$

Combine the SDEs of N targets in (14) and the joint-target state SDE can be characterized as

$$dX_t = AX_t dt + H_N dt + D_N dM_t, \tag{20}$$

where $X_t = [p_{t,x}^{(1)}, v_{t,x}^{(1)}, p_{t,y}^{(1)}, v_{t,y}^{(1)}, \ldots, p_{t,x}^{(N)}, v_{t,x}^{(N)}, p_{t,y}^{(N)}, v_{t,y}^{(N)}]^\top$, $H_N = [0, r_{t,x}^{(1)}(p_{t,x}), 0, r_{t,y}^{(1)}(p_{t,y}), \ldots, 0, \quad r_{t,x}^{(N)}(p_{t,x}), \quad 0, r_{t,y}^{(N)}(p_{t,y})]^\top$ is the repulsive force vector, M_t is a Brownian motion with covariance matrix

$$Q_m = diag[\delta_x^2, \delta_y^2, \ldots, \delta_x^2, \delta_y^2, \delta_g^2, \delta_g^2], \tag{21}$$

where δ_x and δ_y denote the individual motion noise parameters, and δ_g denotes the group motion noise parameter. Moreover, matrix A is defined as

$$A = \begin{bmatrix} A_1 & A_2 & \cdots & \cdots & A_2 \\ A_2 & A_1 & & & \vdots \\ \vdots & & \ddots & & \vdots \\ \vdots & & & A_1 & A_2 \\ A_2 & \cdots & \cdots & A_2 & A_1 \end{bmatrix}, \tag{22}$$

with

$$A_2 = \begin{bmatrix} 0 & 0 & 0 & 0 \\ \frac{\alpha}{N} & \frac{\beta}{N} & 0 & 0 \\ 0 & 0 & 0 & 0 \\ 0 & 0 & \frac{\alpha}{N} & \frac{\beta}{N} \end{bmatrix}, \tag{23a}$$

$$A_3 = \begin{bmatrix} 0 & 1 & 0 & 0 \\ -\alpha & -\beta-\gamma & 0 & 0 \\ 0 & 0 & 0 & 1 \\ 0 & 0 & -\alpha & -\beta-\gamma \end{bmatrix}, \tag{23b}$$

$$A_1 = A_2 + A_3, \tag{23c}$$

and D_N is defined as

$$D_N = \begin{bmatrix} B & C \end{bmatrix}, \tag{24}$$

with

$$B = \begin{bmatrix} B_1 & 0_{4\times2} & \cdots & \cdots & 0_{4\times2} \\ 0_{4\times2} & B_1 & & & \vdots \\ \vdots & & \ddots & & \vdots \\ \vdots & & & B_1 & 0_{4\times2} \\ 0_{4\times2} & \cdots & \cdots & 0_{4\times2} & B_1 \end{bmatrix}, \tag{25a}$$

$$C = [B_1^\top, \ldots, B_1^\top]^\top, \tag{25b}$$

$$B_1 = \begin{bmatrix} 0 & 1 & 0 & 0 \\ 0 & 0 & 0 & 1 \end{bmatrix}^\top. \tag{25c}$$

According to the derivation in [7], the transition function of joint-target state X_t can be expressed by

$$f(X_{t+\tau}|X_t) = \mathcal{N}(e^{A\tau}X_t + R_N H_N, Q_N), \tag{26}$$

where

$$R_N = \int_{s=t}^{s=t+\tau} e^{A(t+\tau-s)}ds, \tag{27a}$$

$$Q_N = \int_{s=t}^{s=t+\tau} e^{A(t+\tau-s)} D_N Q_m D_N^\top (e^{A(t+\tau-s)})^\top ds. \tag{27b}$$

Note that matrix R_N can be calculated via direct matrix exponential expansion [45] or eigenvalue decomposition [46] and Q_N is the covariance matrix.

D. CS Divergence

Given two RFSs, their CS divergence with respective (square integrable) belief densities ϕ and φ, in terms of the set integral, is computed by [38]

$$D_{\mathrm{CS}}(\phi,\varphi) = -\ln \frac{\int K^{|X|}\phi(X)\varphi(X)\delta X}{\sqrt{\int K^{|X|}\phi^2(X)\delta X \int K^{|X|}\varphi^2(X)\delta X}}, \tag{28}$$

where K is the unit of hyper-volume in state space $\mathcal{X}$, and $|X|$ denotes the number of elements in a set X.

To be more specific, if the RFS is subject to *Poisson point process* (PPP), the CS divergence can be further simplified as the following form [33]:

$$D_{\mathrm{CS}}(\phi,\varphi) = \frac{K}{2}||D_\phi(x) - D_\varphi(x)||^2, \tag{29}$$

where $D_\phi(\cdot)$ and $D_\varphi(\cdot)$ are the intensity functions of ϕ and φ respectively, and $||\cdot||^2$ denotes the square of Euclidean norm. Note that the expression in (29) is easy to compute either for GM [34] or *sequential Monte Carlo* (SMC) [36] implementations. Further, for those RFSs who do not admit a closed form to obtain the CS divergence, e.g., MB/PMBM RFSs, an optional method is to compute their PHDs and then substitute them into (29), which is computationally effective to evaluate the discrepancy and has been successfully applied in some sensor control scenarios [36], [37].

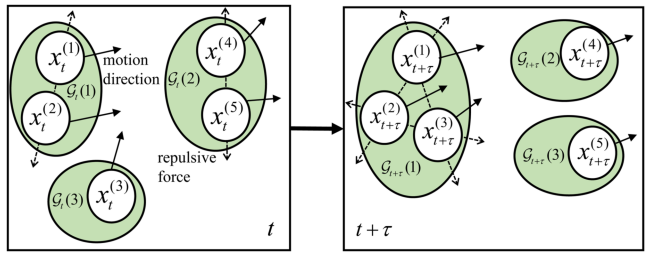

Fig. 1. The change of group structure from time t to time $t+\tau$. $\mathcal{G}_t(g)$ denotes the g-th group at time t, '$\rightarrow$' and '$\dashrightarrow$' denote the motion direction and repulsive force respectively.

III. The Proposed SSTF-MB Filter

In this section, we present an exact solution of the SSTF and then apply the derived results to revise the prediction process of standard MB filter in the space of possible group structures (e.g., see Fig. 1). Moreover, some discussions about the proposed SSTF-MB filter are also given.

A. Derivation of SSTF

Considering that the JSTFD-based method in [19] derives the repulsive force vector by some approximations and omits the process noise for each SSTF, here we derive an exact SSTF from the direct integral solution of the single-target state SDE.

Combine the SDEs on both x- and y- axes in (14) and the single-target state SDE can be written by

$$dx_t^{(i)} = A_3 x_t^{(i)}dt + A_4 x_{t,g}dt + H_t^{(i)}dt + DdM_t, \tag{30}$$

where A_3 is defined in (23b), and

$$A_4 = \begin{bmatrix} 0 & 0 & 0 & 0 \\ \alpha & \beta & 0 & 0 \\ 0 & 0 & 0 & 0 \\ 0 & 0 & \alpha & \beta \end{bmatrix}, \tag{31a}$$

$$H_t^{(i)} = \begin{bmatrix} 0 & r_{t,x}^{(i)}(p_{t,x}) & 0 & r_{t,y}^{(i)}(p_{t,y}) \end{bmatrix}^\top, \tag{31b}$$

$$D = \begin{bmatrix} B_1 & B_1 \end{bmatrix}, \tag{31c}$$

M_t is a Brownian motion with covariance matrix

$$Q_0 = diag[\delta_x^2, \delta_y^2, \delta_g^2, \delta_g^2]. \tag{32}$$

Given the single-target state SDE in (30), the SSTF can be derived by integral operation and the derived result is given in Proposition 1.

Proposition 1: Given the single-target state SDE in (30), the corresponding SSTF is given by

$$f(x_{t+\tau}^{(i)}|x_t^{(i)}) = \mathcal{N}(F_\tau x_t^{(i)} + R_{\tau,g} + O_\tau, Q), \tag{33}$$

where

$$F_\tau = e^{A_3\tau}, \tag{34a}$$

$$R_{\tau,g} = \int_{s=t}^{s=t+\tau} e^{A_3(t+\tau-s)} A_4 x_{s,g} ds, \tag{34b}$$

$$O_\tau = \int_{s=0}^{s=\tau} e^{A_3(\tau-s)} ds \times H_t^{(i)}, \tag{34c}$$

$$Q = \int_{s=0}^{s=\tau} e^{A_3(\tau-s)} D Q_0 D^\top \left(e^{A_3(\tau-s)}\right)^\top ds, \tag{34d}$$

A_3 and A_4 are given in (23b) and (31a), respectively, $H_t^{(i)}$ is given in (31b), D and Q_0 are given in (31c) and (32), respectively.

Proof: Multiply $e^{-A_3 t}$ in both sides of (30), and then,

$$e^{-A_3 t} dx_t^{(i)} = e^{-A_3 t} A_3 x_t^{(i)} dt + e^{-A_3 t} A_4 x_{t,g} dt + e^{-A_3 t} H_t^{(i)} dt + e^{-A_3 t} D dM_t.$$

According to $d(e^{-A_3 t} x_t^{(i)}) = e^{-A_3 t} dx_t^{(i)} - e^{-A_3 t} A_3 x_t^{(i)} dt$, we can obtain

$$d(e^{-A_3 t} x_t^{(i)}) = e^{-A_3 t} A_4 x_{t,g} dt + e^{-A_3 t} H_t^{(i)} dt + e^{-A_3 t} D dM_t.$$

Integrating in terms of s from time t to time $t+\tau$,

$$\int_{s=t}^{s=t+\tau} d(e^{-A_3 s} x_s^{(i)}) = \int_{s=t}^{s=t+\tau} e^{-A_3 s} A_4 x_{s,g} ds + \int_{s=t}^{s=t+\tau} e^{-A_3 s} H_s^{(i)} ds + \int_{s=t}^{s=t+\tau} e^{-A_3 s} D dM_s,$$

and utilizing

$$\int_{s=t}^{s=t+\tau} d(e^{-A_3 s} x_s^{(i)}) = e^{-A_3(t+\tau)} x_{t+\tau}^{(i)} - e^{-A_3 t} x_t^{(i)},$$

we can obtain the following result

$$x_{t+\tau}^{(i)} = e^{A_3 \tau} x_t^{(i)} + \int_{s=t}^{s=t+\tau} e^{A_3(t+\tau-s)} A_4 x_{s,g} ds + \int_{s=t}^{s=t+\tau} e^{A_3(t+\tau-s)} H_t^{(i)} ds + \int_{s=t}^{s=t+\tau} e^{A_3(t+\tau-s)} D dM_s.$$

Further, assuming that the repulsive force is a fixed constant value during $[t, t+\tau)$ and computed based on state configuration at time t and utilizing

$$\int_{s=t}^{s=t+\tau} e^{A_3(t+\tau-s)} ds = \int_{s=0}^{s=\tau} e^{A_3(\tau-s)} ds,$$

$x_{t+\tau}^{(i)}$ can further expressed by

$$x_{t+\tau}^{(i)} = e^{A_3 \tau} x_t^{(i)} + \int_{s=t}^{s=t+\tau} e^{A_3(t+\tau-s)} A_4 x_{s,g} ds + \int_{s=0}^{s=\tau} e^{A_3(\tau-s)} ds \times H_t^{(i)} + \int_{s=t}^{s=t+\tau} e^{A_3(t+\tau-s)} D dM_s.$$

Thus, the distribution of $x_{t+\tau}^{(i)}$ can be returned by a normal form as shown in (33). □

It can be found that the SSTF $f(x_{t+\tau}^{(i)} | x_t^{(i)})$ not only depends on the individual target state $x_t^{(i)}$, but also the state of group center $x_{s,g}$ during time interval $[t, t+\tau)$, which is coupled in the computation of $R_{\tau,g}$. In order to obtain $R_{\tau,g}$, the GSTF needs to be derived, and the derived result is given in the following Proposition 2.

Proposition 2: Given the single-target state SDEs of N targets in (30), the corresponding GSTF is given by

$$f(x_{t+\tau,g} | x_{t,g}) = \mathcal{N}(F_{\tau,g} x_{t,g}, Q_g), \tag{35}$$

where

$$F_{\tau,g} = e^{E\tau}, \tag{36a}$$

$$x_{t,g} = \frac{1}{N} \sum_{i=1}^{N} x_t^{(i)}, \tag{36b}$$

$$Q_g = \int_{s=0}^{s=\tau} e^{E(\tau-s)} D Q_0 D^\top \left(e^{E(\tau-s)}\right)^\top ds, \tag{36c}$$

$$E = \begin{bmatrix} 0 & 1 & 0 & 0 \\ 0 & -\gamma & 0 & 0 \\ 0 & 0 & 0 & 1 \\ 0 & 0 & 0 & -\gamma \end{bmatrix}. \tag{36d}$$

Proof: Sum all single-target state SDEs in (30) and then we have

$$d\left(\sum_{i=1}^{N} x_t^{(i)}\right) = A_3 \left(\sum_{i=1}^{N} x_t^{(i)}\right) dt + N \cdot A_4 x_{t,g} dt + \sum_{i=1}^{N} H_t^{(i)} dt + N \cdot D dM_t.$$

Due to the interaction force for any two targets, thus

$$\sum_{i=1}^{N} H_t^{(i)} = 0.$$

Divide N in both sides and then we can obtain

$$d\left(\frac{1}{N}\sum_{i=1}^{N} x_t^{(i)}\right) = A_3 \left(\frac{1}{N}\sum_{i=1}^{N} x_t^{(i)}\right) dt + A_4 x_{t,g} dt + D dM_t.$$

According to the definitions in (16), we have

$$x_{t,g} = \frac{1}{N}\sum_{i=1}^{N} x_t^{(i)}.$$

Let $E = A_3 + A_4$ and then $dx_{t,g}$ can be expressed by

$$dx_{t,g} = E x_{t,g} dt + D dM_t.$$

Multiplying e^{-Et} in both sides and integrating in terms of s from time t to time $t+\tau$, we can obtain

$$\int_{s=t}^{s=t+\tau} e^{-Es} dx_{s,g} = \int_{s=t}^{s=t+\tau} e^{-Es} E x_{s,g} ds + \int_{s=t}^{s=t+\tau} e^{E(t+\tau-s)} D dM_s.$$

After some simplifications, we can further obtain the following result

$$x_{t+\tau,g} = e^{E\tau} x_{t,g} + \int_{s=t}^{s=t+\tau} e^{E(t+\tau-s)} D dM_s.$$

Thus, the distribution of $x_{t+\tau,g}$ can be returned by a normal form as shown in (35). □

Remark 1: For a special case where there is only one target in a group, the proposed SSTF will degenerate into a prediction of standard single-target prediction process. From the mathematical expression analysis, omitting the force between targets and setting $\alpha = 0$, $\beta = 0$, $D = B_1$ and $Q_0 = diag[\delta_x^2, \delta_y^2]$, the expression in (33) will degenerate into the following form,

$$f(x_{t+\tau}^{(i)}|x_t^{(i)}) = \mathcal{N}(F_\tau x_t^{(i)}, Q), \tag{37}$$

where

$$F_\tau = e^{E\tau}, \tag{38a}$$

$$Q = \int_{s=0}^{s=\tau} e^{E(\tau-s)} B_1 Q_0 B_1^\top \left(e^{E(\tau-s)}\right)^\top ds. \tag{38b}$$

Remark 2: From (35), it can be found that the GSTF does not involve the repulsive force. It is true that the repulsive force comes from internal and is not reflected in the group. Besides, seeing (35) and (37), we can find the GSTF is similar to that of the individual target. Thus, the motion of group center can be seen as the motion of a larger rigid body which consists of many individual targets. On the other hand, the process noise of the group center, compared to the individual target, also considers the noise parameter of group motion in addition to the noise parameters of individual motion.

B. The Prediction Process of SSTF-MB Filter

Firstly, it is emphasized that we only focus on the effect of group structure on the prediction process, not on the update process (discussion will be given later), so that the update process of the proposed SSTF-MB filter is similar to that of the standard MB filter. Meanwhile, the motions of different groups are assumed mutually independent, so that the prediction process can be implemented in parallel.

Then, we define $\mathcal{G}$ as the set of groups with $|\mathcal{G}|$ denoting the cardinality of groups, and the MB density at time t can be expressed by

$$\pi_t = \cup_{g=1}^{|\mathcal{G}|} \{(r_{t,g}^{(i)}, p_{t,g}^{(i)})\}_{i=1}^{N_{t,g}}. \tag{39}$$

Comparing (8) with (39), the difference is that each target in (39) has a corresponding group, which is crucial to the subsequent prediction process.

Moreover, GM approximations [47] are adopted as the implementation tool, so that the i-th target in the g-th group after the filtering process is represented as the following GM form:

$$p_{t,g}^{(i)}(x) = \sum_{a=1}^{J_{t,g}^{(i)}} w_{t,g}^{(i,a)} \mathcal{N}(x; x_{t,g}^{(i,a)}, P_{t,g}^{(i,a)}), \tag{40}$$

where $J_{t,g}^{(i)}$ denotes the number of *Gaussian components* (GCs), $w_{t,g}^{(i,a)}$, $x_{t,g}^{(i,a)}$ and $P_{t,g}^{(i,a)}$ are, respectively, the weight, mean and covariance of the a-th GC.

Further, how to implement the targets grouping is an important issue (implementation method will be discussed later). In general, the distance (e.g., Mahalanobis distance) between targets is always required to compute, which is the basis of grouping. For convenience of calculation, an alternative is to convert the GM form to a single GC form by the following moment-match technology:

$$p_{t,g}^{(i)}(x) \approx w_{t,g}^{(i)} \mathcal{N}(x; \bar{x}_{t,g}^{(i)}, \bar{P}_{t,g}^{(i)}), \tag{41}$$

where $w_{t,g}^{(i)} = 1$ and

$$\bar{x}_{t,g}^{(i)} = \sum_{a=1}^{J_{t,g}^{(i)}} w_{t,g}^{(i,a)} x_{t,g}^{(i,a)}, \tag{42a}$$

$$\bar{P}_{t,g}^{(i)} = \sum_{a=1}^{J_{t,g}^{(i)}} w_{t,g}^{(i,a)} \left[P_{t,g}^{(i,a)} + (x_{t,g}^{(i,a)} - \bar{x}_{t,g}^{(i)})(x_{t,g}^{(i,a)} - \bar{x}_{t,g}^{(i)})^\top\right]. \tag{42b}$$

Based on the approximation in (41), the prediction process of the proposed SSTF-MB filter is given in the following Proposition 3.

Proposition 3: Suppose that the group structure at time t has been obtained, the MB density is given in (39) and each target density is an approximated GC form given in (41), then, the predicted MB density can be represented by

$$\begin{aligned}\pi_{t+\tau|t} = & \cup_{g=1}^{|\mathcal{G}|} \left\{(r_{P,t+\tau|t,g}^{(i)}, p_{P,t+\tau|t,g}^{(i)})\right\}_{i=1}^{N_{t,g}} \\ & \cup \left\{(r_{\Gamma,t+\tau}^{(i)}, p_{\Gamma,t+\tau}^{(i)})\right\}_{i=1}^{N_{\Gamma,t+\tau}},\end{aligned} \tag{43}$$

where $\{(r_{\Gamma,t+i}^{(i)}, p_{\Gamma,t+\tau}^{(i)})\}_{i=1}^{N_{\Gamma,t+\tau}}$ are the newborn target model, while

$$r_{P,t+\tau|t,g}^{(i)} = P_{S,t} r_{t,g}^{(i)}, \tag{44a}$$

$$p_{P,t+\tau|t,g}^{(i)}(x) = w_{t+\tau|t,g}^{(i)} \mathcal{N}(x; x_{t+\tau|t,g}^{(i)}, P_{t+\tau|t,g}^{(i)}), \tag{44b}$$

where $P_{S,t}$ is the survival probability, $w_{t+\tau|t,g}^{(i)} = 1$ and

$$x_{t+\tau|t,g}^{(i)} = F_\tau \bar{x}_{t,g}^{(i)} + R_{\tau,g} + O_\tau, \tag{45a}$$

$$P_{t+\tau|t,g}^{(i)} = F_\tau \bar{P}_{t,g}^{(i)} F_\tau^\top + Q, \tag{45b}$$

where F_τ, $R_{\tau,g}$, O_τ and Q are, respectively, defined in (34a)-(34d).

Remark 3: When all targets follow the motion model in (37), the SSTF-MB filter will degenerate into the standard MB filter. That is to say, the standard MB filter is a special case of the SSTF-MB filter. Hence, if we can know in advance that there is no group targets in the monitored scenario, then the standard MB filter can be directly adopted.

C. Some Discussions

From the description in Section III-B, it can be seen that the group structure plays an important role in the prediction process of SSTF-MB filter. More appropriately, the precise group structure estimate is a premise to ensure the validity of the prediction process. Besides, the group structure can also assist in the measurement update process. Next, the following two discussions about the group structure are pointed out:

Algorithm 1. The SSTF-MB Filter Procedure.

INPUT: $\{(r_t^{(i)}, p_t^{(i)})\}_{i=1}^{N_t}$, $\{(r_{\Gamma,t+\tau}^{(i)}, p_{\Gamma,t+\tau}^{(i)})\}_{i=1}^{N_{\Gamma,t+\tau}}$, $Z_{t+\tau}$.
Target grouping $\rightarrow \mathcal{G}$ and $N_{t,g}, \forall g \in \mathcal{G}$;
Prediction:
for *each* $g \in \mathcal{G}$ **do**
  for *each* $i \in N_{t,g}$ **do**
    Perform SSTF;
  end
end
Merge all predictions and newborn targets;
Perform update based on measurement set $Z_{t+\tau}$**;**
OUTPUT: $\{(r_{t+\tau}^{(i)}, p_{t+\tau}^{(i)})\}_{i=1}^{N_{t+\tau}}$.

- Undirected graph theory, in which each target is regarded as a vertex and the relations between targets are reflected by the edges, can be used to represent each group with a separate graph. A feasible approach is to firstly compute the Mahalanobis distance between targets, and then obtain the adjacency matrix by comparing the computed Mahalanobis distance with the pre-set threshold. More details can be found in [3], [6]. Moreover, the measurement set partitioning strategy adopted in the extended target tracking scenarios [48], [49] can also be considered to generate target groups.
- As a matter of fact, the received measurements are also affected by the group structure. For example, the spatial relative positions between measurements are similar to the spatial relative positions between predicted states. In the usual processing, Mahalanobis distance is used to compute the matching probability between the predicted state and measurement. But for the RGTT, the distance is small so that the correct match is difficult to guarantee. In such a case, if the group structure information (e.g., relative position) is considered, the correct matching probability can be further improved. Currently, some hypergraph-based approaches have been proposed to make use of the group structure during the measurement-update process [50].

Moreover, a pseudo-code of the SSTF-MB filter is given in Algorithm 1.

IV. The Proposed SC-SSTF-MB filter

Notice that the proposed SSTF-MB filter does not consider the scene where the sensor can be mobile. As a matter of fact, whether the trajectory of mobile sensor is reasonable or not has a great influence on the RGTT performance. In this section, we are committed to solve the sensor control problem under the RGTT scenario. Firstly, the problem statement is given, and then the objective function based on CS divergence is formulated. Lastly, the proposed SC-SSTF-MB filter is detailed.

A. Problem Statement

The sensor control problem can be formally cast in the framework of following 6-tuple discrete-time POMDP:

$$\psi = \{X, \mathbb{C}, \mathcal{G}, f(\cdot|\cdot, g), Z, g(\cdot|\cdot, c)\} \tag{46}$$

where $\mathbb{C}$ denotes the sensor control action space, $\mathcal{G}$ denotes the set of groups, $f(\cdot|\cdot, g)$ denotes the SSTF in group $g \in \mathcal{G}$, and $g(\cdot|\cdot, c)$ denotes the single-target likelihood function under the action $c \in \mathbb{C}$.

In the sensor control scenario, some parameters (e.g., the detection probability and measurement noise parameters) are always assumed to be dependent of the relative distance between the target and mobile sensor. In general, the larger the distance, the lower the detection probability and the larger the measurement noise parameters.

Here, we address the problem of controlling the motion direction of mobile sensor with the aim of optimizing the RGTT performance under the consideration of group structure. Our goal is to explore the sensor control strategy in the RGTT scenario by using the proposed SSTF-MB filter and reflect the benefits of considering the group structure.

B. Objective Function Based on CS Divergence

From the perspective of saving computing resources, we resort to computing the CS divergence between two PHDs instead of directly considering two MBs, which has been adopted under the SMC-based implementation [36]. Specifically, the first-order moment (PHD) for $\pi_{1,t}$ characterized by $\{(r_{1,t}^{(i)}, p_{1,t}^{(i)})\}_{i=1}^{J_{1,t}}$ and $\pi_{2,t}$ characterized by $\{(r_{2,t}^{(i)}, p_{2,t}^{(i)})\}_{i=1}^{J_{2,t}}$ is firstly computed via (7). Then, combine the target density approximated by a GC via (41) and the intensity of $\pi_{\ell,t}(x)$ where $\ell = \{1, 2\}$ can be written as

$$D_{\pi_{\ell,t}} = \sum_{i=1}^{J_{\ell,t}} r_{\ell,t}^{(i)} \mathcal{N}(x; \bar{x}_{\ell,t}^{(i)}, \bar{P}_{\ell,t}^{(i)}). \tag{47}$$

Substituting (47) into (29), the resulting expression is given by

$$\begin{aligned} &D_{\mathrm{CS}}(\pi_{1,t}, \pi_{2,t}) \\ &= \frac{K}{2} \sum_{i=1}^{J_{1,t}} \sum_{j=1}^{J_{1,t}} r_{1,t}^{(i)} r_{1,t}^{(j)} \mathcal{N}\left(\bar{x}_{1,t}^{(i)}; \bar{x}_{1,t}^{(j)}, \bar{P}_{1,t}^{(i)} + \bar{P}_{1,t}^{(j)}\right) \\ &\quad + \frac{K}{2} \sum_{i=1}^{J_{2,t}} \sum_{j=1}^{J_{2,t}} r_{2,t}^{(i)} r_{2,t}^{(j)} \mathcal{N}\left(\bar{x}_{2,t}^{(i)}; \bar{x}_{2,t}^{(j)}, \bar{P}_{2,t}^{(i)} + \bar{P}_{2,t}^{(j)}\right) \\ &\quad - K \sum_{i=1}^{J_{1,t}} \sum_{j=1}^{J_{2,t}} r_{1,t}^{(i)} r_{2,t}^{(j)} \mathcal{N}\left(\bar{x}_{1,t}^{(i)}; \bar{x}_{2,t}^{(j)}, \bar{P}_{1,t}^{(i)} + \bar{P}_{2,t}^{(j)}\right). \end{aligned} \tag{48}$$

It can be seen that there are three terms and each term involves evaluations of a Gaussian density within a double sum.

C. Sensor Control Strategy

Based on the POMDP in (46) and objective function in (48), a sensor control strategy coupled with the proposed SSTF-MB filter is further proposed.

Firstly, some necessary explanations of symbols are given as follows.

- H is the length of horizon;
- T is the sampling rate of sensor;

- $\pi_t(X)$ is the posterior multi-target density at time t, and here it is also taken as the initial multi-target density;
- $\bar{\pi}_{t+HT}(X)$ is the predicted multi-target density at time $t+HT$ without considering target birth and death;
- $\tilde{Z}_{t+T:T:t+HT}(c)$ is a collection of *predicted ideal measurement-set* (PIMS) [42] from time $t+T$ to time $t+HT$ under the control action c;
- $\pi_{t+HT}(X|\tilde{Z}_{t+T:T:t+HT}(c))$ is the pseudo updated multi-target density under control action c at time $t+HT$.

Then, the specific sensor control procedures at time t are given by the following five steps.

1) Repeated Prediction: Firstly, find the adjacency matrix between targets so that all targets can be divided some groups. Note that the group target is exactly the individual target when there is only one target within the group. Then, for each group, compute the predicted multi-target density at time $t+HT$ by carrying out the repeated prediction steps (for the case of no target birth or death) of either standard MB filter when only one target exists or SSTF-MB filter when there are at least two targets. Lastly, merge the computed predictions at time $t+HT$ from all groups and denote the predicted MB as $\bar{\pi}_{t+HT|t}(X)$, which is one of the input in the later computation process of CS divergence.

2) Generate PIMS: Firstly, extract the state estimates for each group by selecting those Bernoulli component whose existing probability is larger than a threshold, e.g., $r^{(i)} > 0.5$. Next, for each control action c and each group g, generate the future sets of idealized measurements[3] $\tilde{Z}_{t+T:T:t+HT}(c,g)$. Combine all idealized measurement sets under the same control action,

$$\tilde{Z}_{t+T:T:t+HT}(c) = \bigcup_{g} \tilde{Z}_{t+T:T:t+HT}(c,g). \tag{49}$$

3) Run the SSTF-MB Filter Recursion: Run the SSTF-MB filter (also without target birth and death) with initial multi-target distribution $\pi_t(X)$ using the generated PIMS $\tilde{Z}_{t+T:T:t+HT}(c)$ to get the pseudo updated distribution $\pi_{t+HT}(X|\tilde{Z}_{t+T:T:t+HT}(c))$, which is another input in the later computation process of CS divergence.

4) Compute the Objective Function: For each control action c, substitute $\bar{\pi}_{t+HT|t}(X)$ and $\pi_{t+HT}(X|\tilde{Z}_{t+T:T:t+HT}(c))$ into (48) and then compute the corresponding CS divergence

$$R(c) = D_{\text{CS}}\left(\bar{\pi}_{t+HT|t}(X), \pi_{t+HT}(X|\tilde{Z}_{t+T:T:t+HT}(c))\right). \tag{50}$$

5) Make Decision: Select the control action with the maximum CS divergence as the next motion direction of sensor:

$$\hat{c} = \max_{c} R(c). \tag{51}$$

Further, a pseudo-code of the SC-SSTF-MB filter is given in Algorithm 2.

Remark 4: The more control actions that $\mathbb{C}$ contains, the more likely it is that the decision made by the sensor will be reasonable. Moreover, The larger the value of H, the longer the future time that sensor needs to consider. From the viewpoint of computation complexity, larger values of H and $|\mathbb{C}|$ also mean that more computational resources are required.

[3]It corresponds to a generation process with noise-free, clutter-free environment and unity detection probability.

TABLE I
SIMULATION PARAMETERS AND THEIR SYMBOLS AND VALUES

Simulation Parameter	Symbol	Value
sampling rate	τ	4 s
survival probability	$P_{S,t}$	0.95
clutter rate	λ_c	20
minimum distance between groups	d	200 m
position control parameter	α	0.005
velocity control parameter	β	0.4
individual velocity control parameter	γ	0.0001
individual motion noise	δ_x, δ_y	3
group motion noise	δ_g	5
repulsive force parameters	R_1	10
	R_2	8

Algorithm 2. The SC-SSTF-MB Filter Procedure.

INPUT: $\{(r_t^{(i)}, p_t^{(i)})\}_{i=1}^{N_t}$, H, T, $\mathbb{C}$.
Repeated prediction:
for $h = 1 : H$ **do**
  if $h = 1$ **then**
    $\pi_t(X) \to \bar{\pi}_{t+T}(X)$
  else
    $\pi_{t+(h-1)T}(X) \to \bar{\pi}_{t+hT}(X)$
  end
end
for *each* $c \in \mathbb{C}$ **do**
  for *each* $g \in \mathcal{G}$ **do**
    Generate PIMS $\to \tilde{Z}_{t+T:T:t+HT}(c,g)$
  end
  Combine all PIMSs:
  $\tilde{Z}_{t+T:T:t+HT}(c) = \bigcup_g \tilde{Z}_{t+T:T:t+HT}(c,g)$
  Run the SSTF-MB filter $\to \pi_{t+HT}(X|\tilde{Z}_{t+T:T:t+HT}(c))$
  Compute the objective function:
  $R(c) = D_{\text{CS}}(\bar{\pi}_{t+HT|t}(X), \pi_{t+HT}(X|\tilde{Z}_{t+T:T:t+HT}(c)))$
end
Make decision: $\hat{c} = \max_c R(c)$.
OUTPUT: $\hat{c}$.

V. PERFORMANCE EVALUATION

In this section, we analyze the tracking performance of the proposed SSTF-MB filter and SC-SSTF-MB filter in two 2-dimensional RGTT scenarios in terms of the OSPA distance [51] with Euclidean distance $p = 1$ and cutoff parameter $c = 100$ m. The targets follow the motion model in (33) and the sensor (e.g., radar) measures the target bearing and range, where the measurement dependent of the target position $x_t = [p_{t,x}, p_{t,y}]$ and sensor position $u_t = [s_{t,x}, s_{t,y}]$ at time t is given by

$$z_t = \begin{bmatrix} \arctan(\frac{p_{t,y}-s_{t,y}}{p_{t,x}-s_{t,x}}) \\ \sqrt{(p_{t,x}-s_{t,x})^2 + (p_{t,y}-s_{t,y})^2} \end{bmatrix} + w_t, \tag{52}$$

where $w_t \sim \mathcal{N}(\cdot; 0, R_t)$ is the measurement noise with covariance $R_t = diag(\sigma_\theta^2, \sigma_r^2)$ with σ_θ and σ_r denoting the standard deviations of bearing and range, respectively. Moreover, the other parameters are listed in Table I. Further, all simulation results are averaged by 100 independent *Monte Carlo* (MC) runs.

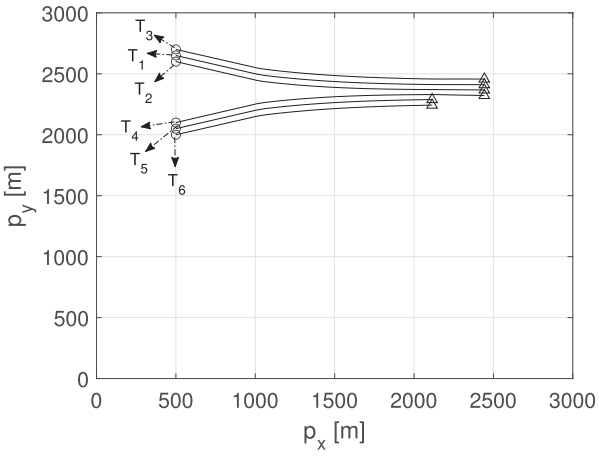

Fig. 2. The simulation scenario 1 consisting of six targets, where starting/ending points for each trajectory are shown with $\circ/\triangle$.

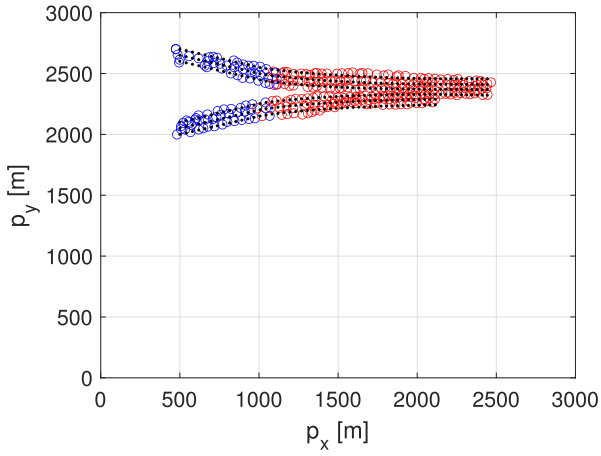

Fig. 3. The estimated positions of targets in a typical experiment wherein the blue and red circles represent estimates from two different groups and one group, respectively.

A. Scenario 1

To intuitively demonstrate the effectiveness of SSTF-MB filter and SC-SSTF-MB filter, a simple scenario involving six targets, which are monitored for 220 s, in the surveillance region $[0, 3000] \times [0, 3000]$ (in m^2) is considered as shown in Fig. 2. The initial states of these targets are $x^{(1)} = [500, 10, 2650, -3]^\top$, $x^{(2)} = [500, 10, 2600, -3]^\top$, $x^{(3)} = [500, 10, 2700, -3]^\top$, $x^{(4)} = [500, 10, 2100, 3]^\top$, $x^{(5)} = [500, 10, 2050, 3]^\top$, $x^{(6)} = [500, 10, 2000, 3]^\top$. Moreover, the time-varying group information is set as follows:

- two separate groups, $\{\mathrm{T}_1, \mathrm{T}_2, \mathrm{T}_3\}$ and $\{\mathrm{T}_4, \mathrm{T}_5, \mathrm{T}_6\}$, travel independently during [1,48) s;
- two groups are merged into one group as $\{\mathrm{T}_1, \mathrm{T}_2, \mathrm{T}_3, \mathrm{T}_4, \mathrm{T}_5, \mathrm{T}_6\}$ during [48,190] s;
- targets $\{\mathrm{T}_5, \mathrm{T}_6\}$ disappear and one group $\{\mathrm{T}_1, \mathrm{T}_2, \mathrm{T}_3, \mathrm{T}_4\}$ travels during (190,220] s.

In the implementation, the method in [6] is adopted to achieve the estimate of target grouping.

1) Case 1: Firstly, the effectiveness of the proposed SSTF-MB filter is compared with the standard MB filter wherein each target follows the motion model in (37), JSTFD-MB filter [19] and *TOGC-based MB* (TOGC-MB) filter [6]. The common parameters are set as follows:

- The platform is time-invariant and sensor is located at $u_t = [1500, 500]$ m;
- The detection probability is assumed to be constant with $P_{D,t} = 0.90$;
- The scales of range and bearing noise are $\sigma_r = 5$ m and $\sigma_\theta = 1^o$, respectively.

Fig. 3 shows the estimated positions of targets for the proposed SSTF-MB filter in one MC wherein the blue and red circles represent estimates from two different groups and one group, respectively. It shows that two independent groups move separately and then they are combined into one group when the distance threshold is satisfied.

From Fig. 4, it can be seen that the tracking performance of the TOGC-MB filter, JSTFD-MB filter and the proposed SSTF-MB filter are better than that of the standard MB filter due to the consideration of group structure information. Moreover, the proposed SSTF-MB filter performs also better than the TOGC-MB filter and JSTFD-MB filter. This is because the motion model of the proposed SSTF-MB filter is more precise.

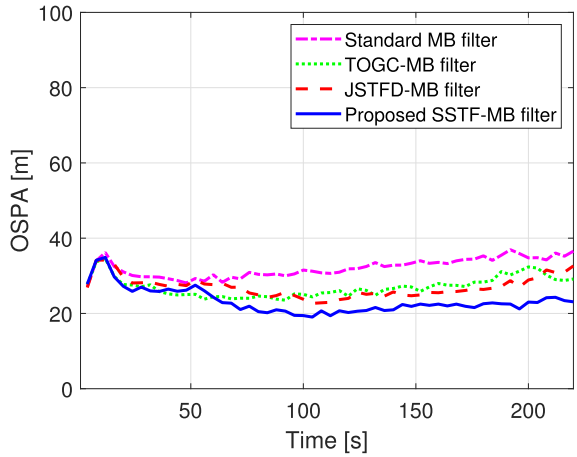

Fig. 4. The OSPA error comparison between the standard MB filter, TOGC-MB filter, JSTFD-MB filter and proposed SSTF-MB filter in scenario 1.

2) Case 2: A mobile sensor platform is considered to compare the tracking performance between the proposed SC-SSTF-MB filter and other approaches including *random selection based on SSTF-MB* (RS-SSTF-MB) filter and *sensor control based on the standard MB* (SC-MB) filter. The initial position of sensor is [1500,500] m and the sensor's velocity is constant with 10 m/s but the course is changeable. Total space is discretized at 30^o intervals so that the allowable course changes are

$$\mathbb{C} = [-180^\circ, -150^\circ, \ldots, 0^\circ, \ldots, 150^\circ, 180^\circ]. \tag{53}$$

Moreover, the idealized measurements are generated over a horizon length of $H = 2$ and sampling period $T = 20$ s, so that there are five adjustments for the sensor at time 40 s, 80 s, 120 s, 160 s, and 220 s. Further, the scales of range and bearing noise are assumed

$$\sigma_r = \sigma_0 + \eta_r \|x_t - u_t\|^2, \tag{54}$$

$$\sigma_\theta = \theta_0 + \eta_\theta \|x_t - u_t\|, \tag{55}$$

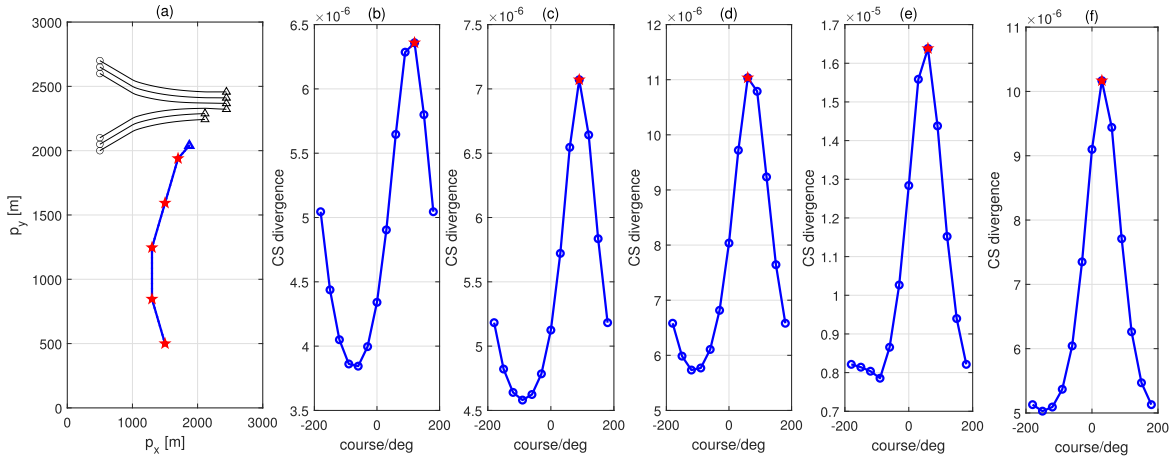

Fig. 5. The left sub-figure (a) shows the sensor trajectory from a typical run for the SC-MB filter, and the other sub-figures (b)-(f) are the corresponding five selected courses represented by '★'.

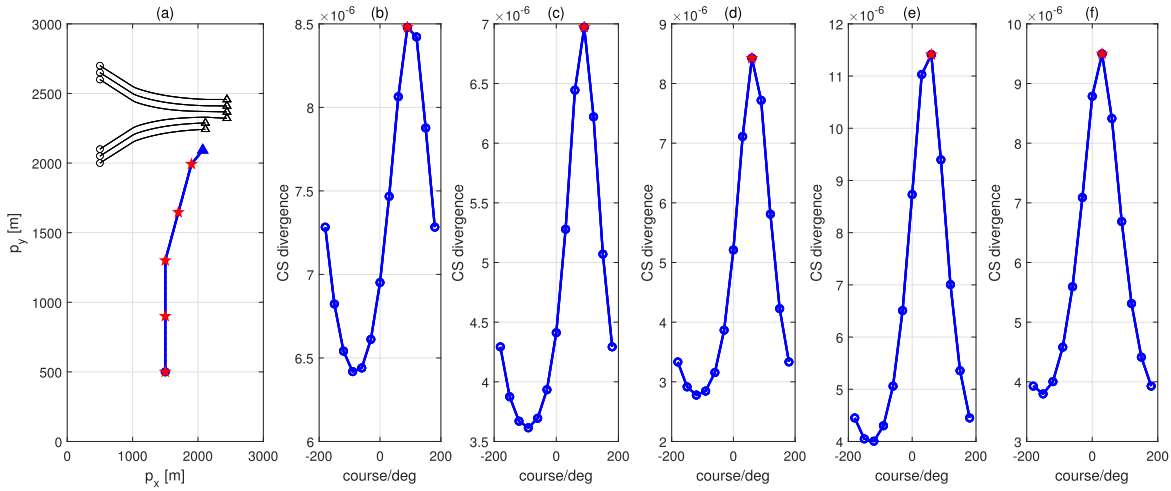

Fig. 6. The left sub-figure (a) shows the sensor trajectory from a typical run for the SC-SSTF-MB filter, and the other sub-figures (b)-(f) are the corresponding five selected courses represented by '★'.

where $\sigma_0 = 5\,\text{m}, \eta_r = 5 \times 10^{-5}\,m^{-1}, \theta_0 = \pi/180\,\text{rad}$ and $\eta_\theta = 5 \times 10^{-6}\,m^{-1}$, and the detection probability is modeled by the following form,

$$P_D(x_t, u_t) = \frac{\mathcal{N}(\|x_t - u_t\|; 0, \sigma_D)}{\mathcal{N}(0; 0, \sigma_D)}, \tag{56}$$

where $\sigma_D = 5000$ m controls the rate at which the detection probability drops off as the range increases.

Firstly, to intuitively show the tracking difference between the SC-MB filter and SC-SSTF-MB filter, Fig. 5 and Fig. 6, respectively, show the sensor's trajectory and corresponding computed CS divergence as well as the selected courses. It can be found that the adjustment of SC-SSTF-MB filter makes the sensor move closer to the group target comparing to the SC-MB filter.

Moreover, the comparison of tracking performance between the SC-MB filter, RS-SSTF-MB filter and proposed SC-SSTF-MB filter, in terms of average OSPA error, is provided in Fig. 7. It indicates that

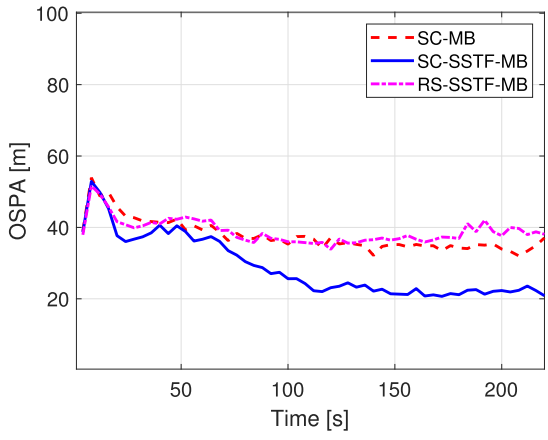

Fig. 7. The average OSPA error comparison between the SC-MB filter, RS-SSTF-MB filter and proposed SC-SSTF-MB filter in scenario 1.

- the RS-SSTF-MB filter is sometimes worse than the SC-MB filter, this is because that the randomness of the selected course makes the filtering parameters worse, i.e.,

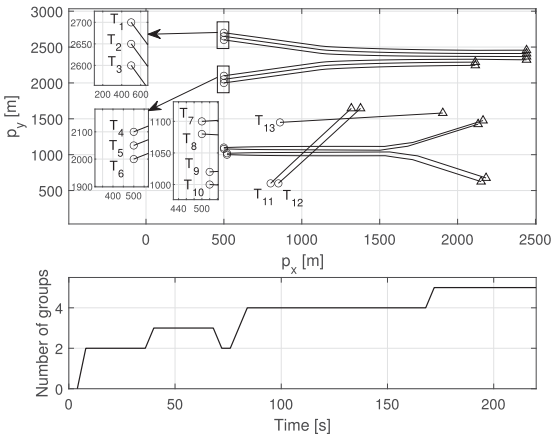

Fig. 8. (a) The simulation scenario 2 consisting of thirteen targets where starting/ending points for each trajectory are shown with ○/△. (b) True number of groups.

TABLE II
NEWBORN TARGETS INFORMATION

Target ID	Init. Loc (m)	Init. Velo. (m/s)	Birth/Death (s)
T_1	$[500, 2650]$	$[10, -3]$	$1/220$
T_2	$[500, 2600]$	$[10, -3]$	$1/220$
T_3	$[500, 2700]$	$[10, -3]$	$1/220$
T_4	$[500, 2100]$	$[10, 3]$	$1/220$
T_5	$[500, 2050]$	$[10, 3]$	$1/180$
T_6	$[500, 2000]$	$[10, 3]$	$1/180$
T_7	$[500, 1100]$	$[10, 0]$	$40/220$
T_8	$[500, 1080]$	$[10, 0]$	$40/220$
T_9	$[520, 1020]$	$[10, 0]$	$40/220$
T_{10}	$[520, 1000]$	$[10, 0]$	$40/220$
T_{11}	$[800, 600]$	$[4, 8]$	$80/220$
T_{12}	$[850, 600]$	$[4, 8]$	$80/220$
T_{13}	$[860, 1450]$	$[8, 1]$	$80/220$

smaller detection probability and larger measurement noise parameters.

- the proposed SC-SSTF-MB filter always outperforms both the SC-MB filter and RS-SSTF-MB filter at the lower OSPA error, which shows the superiority of considering both sensor control strategy and group structure information.

B. Scenario 2

To further assess the performance of the proposed SSTF-MB filter and SC-SSTF-MB filter, a more challenging scenario with thirteen targets involving single-target and target splitting as well as target merging is considered as shown in Fig. 8(a), and the corresponding time-varying number of groups is shown in Fig. 8(b). The involved newborn targets information is listed in Table II.

1) Case 1: Here, the proposed SSTF-MB filter is tested. Firstly, the estimated number of groups for the SSTF-MB filter is given in Fig. 9. It shows that the groups can be estimated accurately, even if there is some time delay when target merging or splitting happens. Moreover, the OSPA error comparison between the proposed SSTF-MB filter and other approaches is shown in Fig. 10. It turns out that the proposed SSTF-MB filter also provides the best tracking performance even in the complex tracking scenario.

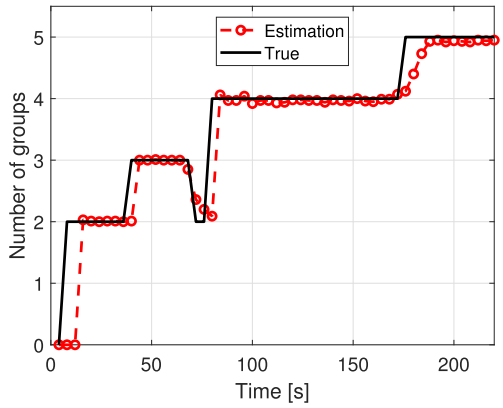

Fig. 9. The estimated number of groups in scenario 2.

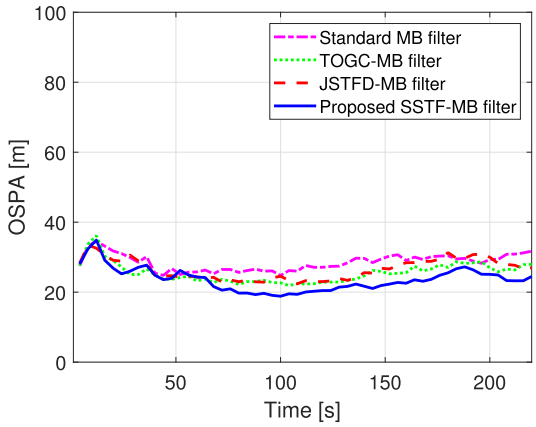

Fig. 10. The OSPA error comparison between the standard MB filter, TOGC-MB filter, JSTFD-MB filter and proposed SSTF-MB filter in scenario 2.

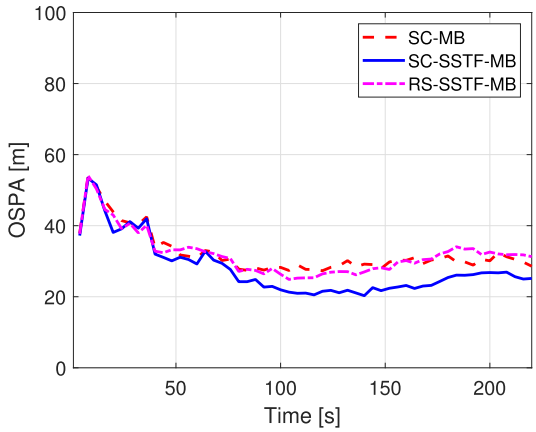

Fig. 11. The OSPA error comparison between the SC-MB filter, RS-SSTF-MB filter and SC-SSTF-MB filter in scenario 2.

2) Case 2: The proposed SC-SSTF-MB filter is tested where the parameter settings of the mobile sensor are the same as those in case 2 of scenario 1, and the resulting OSPA error comparison between the SC-MB filter, RS-SSTF-MB filter and SC-SSTF-MB filter is shown in Fig. 11. It shows that the proposed SC-SSTF-MB filter still obtains better tracking performance than other approaches.

VI. Conclusion and Future Works

In this paper, we proposed a new multi-Bernoulli (MB) filter to solve the *resolvable group target tracking* (RGTT) problem by deriving the *single-target state transition function* (SSTF), called SSTF-MB. Then, applying the proposed SSTF-MB filter into the sensor control scenario, we proposed a sensor control based on the SSTF-MB filter, called SC-SSTF-MB, to assist the mobile sensor to select the optimal control action and obtain good tracking performance. Simulation experiments demonstrated the effectiveness and superiority of the proposed SSTF-MB filter and SC-SSTF-MB filter.

In the future work, three possible topics will be considered:

- the proposed SSTF can be applied to the labeled filters [16], [17], [18] for the RGTT scenarios where the identities of targets are important.
- the group structure will be considered both in prediction process and measurement-update process to search much better RGTT performance.
- the proposed SC-SSTF-MB filter can be extended to the multi-sensor control scenario [39], [40], [41].

Acknowledgment

The authors would like to thank the anonymous Reviewers and Associate Editor for their many valuable suggestions, which have significantly improved the quality of this paper.

References

[1] R. Mahler, *Statistical Multisource-Multitarget Information Fusion*. Norwood, MA, USA: Artech House, 2007.
[2] X. Hao, Y. Liang, W. Zhang, and L. Xu, "Structure identification and tracking of multiple resolvable group targets with circular formation," in *Proc. IEEE Joint Int. Inf. Technol. Artifi. Intelli. Conf.*, 2020, pp. 910–915.
[3] W. Liu, S. Zhu, C. Wen, and Y. Yu, "Structure modeling and estimation of multiple resolvable group targets via graph theory and multi-Bernoulli filter," *Automatica*, vol. 89, pp. 274–289, Mar. 2018.
[4] Y. Chi and W. Liu, "Resolvable group state estimation with maneuver movement based on labeled RFS," in *Proc. IEEE Int. Conf. Control, Automat. Inf. Sci.*, 2018, pp. 249–254.
[5] Y. Chi and W. Liu, "Resolvable group state estimation with maneuver based on labeled RFS and graph theory," *Sensors*, vol. 19, no. 6, Mar. 2019, Art. no. 1307.
[6] Z. Zhang, J. Sun, H. Zhou, and C. Xu, "Group target tracking based on MS-MeMBer filters," *Remote Sens.*, vol. 13, no. 10, May 2021, Art. no. 1920.
[7] S. K. Pang, J. Li, and S. J. Godsill, "Detection and tracking of coordinated groups," *IEEE Trans. Aerosp. Electron. Sys.*, vol. 47, no. 1, pp. 472–502, Jan. 2011.
[8] J. Wang, H. Yin, and S. Wei, "Group tracking based on hypothesis management aided MCMC-PF algorithm," in *Proc. CIE Int. Conf. Radar*, 2016, pp. 1–5.
[9] Q. Li, S. J. Godsill, J. Liang, and B. I. Ahmad, "Inferring dynamic group leadership using sequential Bayesian methods," in *Proc. IEEE Int. Conf. Acoust. Speech Signal Process.*, 2020, pp. 8911–8915.
[10] Q. Li, B. I. Ahmad, and S. J. Godsill, "Sequential dynamic leadership inference using Bayesian monte carlo methods," *IEEE Trans. Aerosp. Electron. Sys.*, vol. 57, no. 4, pp. 2039–2052, Aug. 2021.
[11] Y. Bar-Shalom and T. Fortmann, *Tracking and Data Association*. Cambridge, MA, USA: Academic Press, 1988.
[12] S. S. Blackman and R. Popoli, *Design and Analysis of Modern Tracking Systems*. Norwood, MA, USA: Artech House, 1999.
[13] R. Mahler, "Multi-target Bayes filtering via first-order multi-target moments," *IEEE Trans. Aerosp. Electron. Syst.*, vol. 39, no. 4, pp. 1152–1178, Oct. 2003.
[14] R. Mahler, "PHD filters of higher order in target number," *IEEE Trans. Aerosp. Electron. Syst.*, vol. 43, no. 3, pp. 1523–1543, Oct. 2007.
[15] B. T. Vo, B. N. Vo, and A. Cantoni, "The cardinality balanced multi-target multi-Bernoulli filter and its implementations," *IEEE Trans. Signal Process.*, vol. 57, no. 2, pp. 409–423, Feb. 2009.
[16] B. T. Vo and B. N. Vo, "Labeled random finite sets and multi-object conjugate priors," *IEEE Trans. Signal Process.*, vol. 61, no. 13, pp. 3460–3475, Jul. 2013.
[17] B. N. Vo, B. T. Vo, and D. Phung, "Labeled random finite sets and the Bayes multi-object tracking filter," *IEEE Trans. Signal Process.*, vol. 62, no. 24, pp. 6554–6567, Dec. 2014.
[18] S. Reuter, B. T. Vo, B. N. Vo, and K. Dietmayer, "The labeled multi-Bernoulli filter," *IEEE Trans. Signal Process.*, vol. 62, no. 12, pp. 3240–3246, Jun. 2014.
[19] L. Li, Q. Wu, B. Yang, S. Wei, and J. Wang, "Labeled multi-Bernoulli filter based group target tracking using SDE and graph theory," in *Proc. Int. Conf. Inf. Fusion*, 2021, pp. 1–8.
[20] A. Gning, L. Mihaylova, S. Maskell, S. K. Pang, and S. Godsill, "Group object structure and state estimation with evolving networks and Monte Carlo methods," *IEEE Trans. Signal Process.*, vol. 59, no. 4, pp. 1383–1396, Apr. 2011.
[21] D. P. Bertsakes, *Dynamic Programming and Optional Control*. Nashua, NH, USA: Athena Sci., 1995.
[22] G. E. Monahan, "A survey of partially observable Markov decision process: Theory, models and algorithms," *Manage. Sci.*, vol. 28, no. 1, pp. 1–16, Jan. 1982.
[23] H. G. Hoang and B. T. Vo, "Sensor management for multi-target via multi-Bernoulli filtering," *Automatica*, vol. 50, no. 4, pp. 1135–1142, Apr. 2014.
[24] A. K. Gostar, R. Hoseinnezhad, and A. Bab-Hadiashar, "Multi-Bernoulli sensor control for multi-target tracking," in *Proc. IEEE Int. Conf. Intelli. Sensors Sensor Netw. Inf. Process.*, 2013, pp. 312–317.
[25] Y. Zhu, J. Wang, and S. Liang, "Multi-objective optimization based multi-Bernoulli sensor selection for multi-target tracking," *Sensors*, vol. 19, no. 4, pp. 1–18, Feb. 2019.
[26] A. K. Gostar, R. Hoseinnezhad, and A. Bab-Hadiashar, "Robust multi-Bernoulli sensor selection for multi-target tracking in sensor networks," *IEEE Signal Process. Lett.*, vol. 20, no. 12, pp. 1167–1170, Dec. 2013.
[27] A. K. Gostar, R. Hoseinnezhad, and A. Bab-Hadiashar, "Multi-Bernoulli sensor control via minimization of expected estimation errors," *IEEE Trans. Aerosp. Electron. Sys.*, vol. 51, no. 3, pp. 1762–1773, Jul. 2015.
[28] A. K. Gostar, R. Hoseinnezhad, A. Bab-Hadiashar, and W. Liu, "Sensor-management for multitarget filters via minimization of posterior dispersion," *IEEE Trans. Aerosp. Electron. Sys.*, vol. 53, no. 6, pp. 2877–2884, Dec. 2017.
[29] K. Kastellla, "Discrimination gain to optimize detection and classification," *IEEE Trans. Syst. Man, Cyber. - Part A: Syst. Hum.*, vol. 27, no. 1, pp. 112–116, Jan. 1997.
[30] B. Ristic and B. N. Vo, "Sensor control for multi-object state-space estimation using random finite set," *Automatica*, vol. 46, no. 11, pp. 1812–1818, Nov. 2010.
[31] B. Ristic and S. Arulampalam, "Bearings only tracking in clutter with observer control using the Bernoulli particle filter," in *Proc. Australian Control Conf.*, 2011, pp. 487–492.
[32] A. K. Gostar, R. Hoseinnezhad, and A. Bab-Hadiashar, "Multi-Bernoulli sensor-selection for multi-target tracking with unknown clutter and detection profiles," *Signal Process.*, vol. 119, pp. 28–42, Feb. 2016.
[33] H. G. Hoang, B. N. Vo, B. T. Vo, and R. Mahler, "The Cauchy-Schwarz divergence for Poisson point process," *IEEE Trans. Signal Process.*, vol. 61, no. 8, pp. 4475–4485, Aug. 2015.
[34] Y. Liu and H. G. Hoang, "Sensor selection for multi-target tracking via closed form Cauchy-Schwarz divergence," in *Proc. Int. Conf. Control, Automat. Inf. Sci.*, 2014, pp. 93–98.
[35] M. Beard, B.-T. Vo, B.-N. Vo, and S. Arulampalam, "Sensor control for multi-target tracking using Cauchy-Schwarz divergence," in *Proc. Int. Conf. Inf. Fusion*, 2015, pp. 937–944.
[36] A. K. Gostar, R. Hoseinnezhad, and A. Bab-Hadiashar, "Multi-Bernoulli sensor control using Cauchy-Schwarz divergence," in *Proc. Int. Conf. Inf. Fusion*, 2016, pp. 651–657.
[37] A. K. Gostar, R. Hoseinnezhad, T. Rathnayake, X. Wang, and A. Bab-Hadiashar, "Constrained sensor control for labeled multi-Bernoulli filter using cauchy-schwarz divergence," *IEEE Signal Process. Lett.*, vol. 24, no. 9, pp. 1313–1317, Sep. 2017.
[38] M. Beard, B.-T. Vo, B.-N. Vo, and S. Arulampalam, "Void probabilities and Cauchy–Schwarz divergence for generalized labeled multi-Bernoulli models," *IEEE Trans. Signal Process.*, vol. 65, no. 19, pp. 5047–5061, Oct. 2017.
[39] M. Jiang, W. Yi, and L. Kong, "Multi-sensor control for multi-target tracking using Cauchy-Schwarz divergence," in *Proc. Int. Conf. Inf. Fusion*, 2016, pp. 2059–2066.

[40] G. Li, S. Li, W. Yi, T. Zhou, and L. Kong, "A suboptimal multi-sensor management based on Cauchy-Schwarz divergence for multi-target tracking," in *Proc. Int. Conf. Inf. Fusion*, 2018, pp. 1–8.
[41] Y. Zhu, S. Liang, M. Gong, and J. Yan, "Decomposed POMDP optimization-based sensor management for multi-target tracking in passive multi-sensor systems," *IEEE Sensors J.*, vol. 22, no. 4, pp. 3565–3578, Feb. 2022.
[42] R. Mahler, *Advances in Statistical Multisource-Multitarget Information Fusion*. Norwell, MA, USA: Artech House, 2014.
[43] B. T. Vo, B. N. Vo, and D. Suter, "Joint detection and estimation of multiple objects from image observation," *IEEE Trans. Signal Process.*, vol. 58, no. 10, pp. 5129–5141, Oct. 2010.
[44] S. Särkkä and A. Solin, *Applied Stochastic Differential Equations*. Cambridge, U.K.: Cambridge Univ. Press, 2019.
[45] B. Øksendal, *Stochastic Differential Equations: An Introduction With Applications*. 6th ed. Berlin, Germany: Springer, 2003.
[46] M. A. S. Salman and V. C. Borkar, "Exponential matrix and their properties," *Int. J. Sci. Innov. Math. Res.*, vol. 4, no. 1, pp. 53–63, 2016.
[47] B. N. Vo and W. K. Ma, "The Gaussian mixture probability hypothesis density filter," *IEEE Trans. Signal Process.*, vol. 54, no. 11, pp. 4091–4104, Nov. 2006.
[48] K. Granström and U. Orguner, "A PHD filter for tracking multiple extended targets using random matrices," *IEEE Trans. Signal Process.*, vol. 60, no. 11, pp. 5657–5671, Nov. 2012.
[49] C. Lundquist, K. Granström, and U. Orguner, "An extended target CPHD filter and a gamma Gaussian inverse Wishart implementation," *IEEE J. Sel. Topics Signal Process.*, vol. 7, no. 3, pp. 472–483, Jun. 2013.
[50] H. Yu, W. An, R. Zhu, and R. Guo, "A hypergraph matching labeled multi-Bernoulli filter for group targets tracking," *IEICE Trans. Inf. Sys.*, vol. 102, no. 10, pp. 2077–2081, Oct. 2019.
[51] D. Schuhmacher, B. T. Vo, and B. N. Vo, "A consistent metric for performance evaluation of multi-object filters," *IEEE Trans. Signal Process.*, vol. 56, no. 8, pp. 3447–3457, Aug. 2008.

Guchong Li (Member, IEEE) received the B.S. degree in electrical engineering and the Ph.D. degree in information and communication engineering from the University of Electronic Science and Technology of China, Chengdu, China, in 2016 and 2021, respectively. From October 2018 to October 2020, he was a Visiting Student with the Dipartimento di Ingegneria dell'Informazione, Università di Firenze, Firenze, Italy. He is currently a Postdoctoral Fellow with the Department of Electronic Engineering, Tsinghua University, Beijing, China. His research interests include random finite set, extended/resolvable target tracking, and multi-sensor data fusion.

Gang Li (Senior Member, IEEE) received the B.S. and Ph.D. degrees in electronic engineering from Tsinghua University, Beijing, China, in 2002 and 2007, respectively. Since July 2007, he has been a Faculty Member with Tsinghua University, where he is currently a Professor with the Department of Electronic Engineering. From 2012 to 2014, he visited The Ohio State University, Columbus, OH, USA, and Syracuse University, Syracuse, NY, USA. He has authored or coauthored more than 200 journal articles and conference papers. He has authored the book *Advanced Sparsity-Driven Models and Methods for Radar Applications,* London, U.K., SciTech/IET Publishing, in 2020, and Edited the book *Radar Countermeasures for Unmanned Aerial Vehicles,* London, U.K., SciTech/IET Publishing, in 2021. His research interests include radar signal processing, distributed signal processing, remote sensing, and information fusion. Prof. Li is the Senior Area Editor of the IEEE SIGNAL PROCESSING LETTERS and an Associate Editor for the IEEE JOURNAL OF SELECTED TOPICS IN APPLIED EARTH OBSERVATIONS AND REMOTE SENSING. He was also an Associate Editor for the IEEE TRANSACTIONS ON SIGNAL PROCESSING, Special Sessions Chair for the International Conference on Acoustics, Speech, and Signal Processing 2021, and the Tutorial Speaker for the IEEE Radar Conference 2017.

You He received the Ph.D. degree in electronic engineering from Tsinghua University, Beijing, China, in 1997. He is currently a Professor with Naval Aeronautical University, Yantai, China. He is also cross-appointed with the Department of Electronic Engineering, Tsinghua University. He has authored or coauthored more than 300 academic articles. He is also the author of *Radar Target Detection* and *CFAR Processing*, Tsinghua University Press, Beijing, China, *Multi-Sensor Information Fusion With Applications* and *Radar Data Processing With Applications,* Publishing House of Electronics Industry, Beijing, China. His research interests include detection and estimation theory, CFAR processing, distributed detection theory, and multi-sensor information fusion. He is also the Fellow Member of the Chinese Academy of Engineering. In 2017, he was the recipient of the top prize in science and technology of Shandong Province. He is also on the editorial boards for the *Journal of Data Acquisition and Processing*, *Modern Radar*, *Fire Control and Command Control*, and *Radar Science and Technology*.